Russian Chemical Reviews **68** (5) 381 – 392 (1999) © 1999 Russian Academy of Sciences and Turpion Ltd

UDC 541.148

Synthetic diamond in electrochemistry

Yu V Pleskov

Contents

I.	Introduction	381
II.	Preparation of diamond thin-film electrodes	382
III.	Crystal structure and basic electrophysical characteristics of diamond films	382
IV.	Synthetic diamond films as electrodes: resistance to corrosion and background current – potential curves	383
V.	Impedance spectroscopy and semiconductor properties of diamond electrodes	384
VI.	Kinetics of the electrode reactions	387
VII.	Photoelectrochemistry of diamond	390
VIII.	Conclusion	391

Abstract. The results of studies on the electrochemistry of diamond carried out during the last decade are reviewed. Methods for the preparation, the crystalline structure and the main electro physical properties of diamond thin films are considered. Depending on the doping conditions, the diamond behaves as a superwide-gap semiconductor or as a semimetal. It is shown that the 'metal-like' diamond is corrosion-resistant and can be used advantageously as an electrode in the electrosynthesis (in particular, for the electroreduction of compounds that are difficult to reduce) and electroanalysis. Kinetic characteristics of some redox reactions and the impedance parameters for diamond electrodes are presented. The results of comparative studies of the electrodes made of diamond single crystals, polycrystalline diamond and amorphous diamond-like carbon, which reveal the effect of the crystalline structure (*e.g.*, the influence of intercrystallite boundaries) on the electrochemical properties of diamond, are presented. The bibliography includes 99 references.

I. Introduction

Diamond is a material endowed with unique properties: it is a perfect dielectric characterised by extremely high atomic density and hardness. Historical records of intensive electrophysical, physicochemical and optical studies of diamond is only several-decade long.[1,2] Its practical uses have diversified and embrace nowadays such fields as materials technology,[3] microelectronics [4] and other.

Depending on the doping level, diamond behaves as a superwide-gap semiconductor or as a semimetal. Owing to its exceptional chemical stability, semiconductor diamond is undoubtedly promising as an electrode material. However, in contrast with other carbon materials of long-standing use (graphite, glassy carbon and other), electrochemical studies of diamond were initiated approximately a decade ago. Until recently, such investigations have been seriously hampered by two circumstances: firstly, diamond remained an exotic, difficultly accessible material; secondly, by its nature, diamond is an insulator and hence is unsuitable material for electrodes.

The situation has radically changed in connection with the achievements in the technology of manufacture of diamond thin films from the gas phase under subatmospheric pressure. Highly efficient methods have been developed for the growing of polycrystalline diamond films on non-diamond substrates; such films are relatively inexpensive when manufactured on a large scale. Doping with boron, as an acceptor admixture, allowed one to synthesise semiconductor films with good conductivity, while high doping levels led to quasimetallic films.[5]

The first studies on diamond electrodes have opened a new branch of electrochemistry of semiconductor materials [6] known now as electrochemistry of diamond.

Formally, the first publication on diamond electrochemistry was that describing attempts to make an electrode from a dielectric diamond crystal.[7] In order to make electroconducting at least the thin outer layer of the specimen, the authors implanted Ar^+ ions into the diamond crystal. Argon is not a doping impurity for the diamond and does not change its conductivity, but as the result of such an ion implantation the external diamond layer becomes amorphous (*e.g.*, see Refs 8, 9). A noticeable conductivity arises because of the destruction of the diamond crystalline lattice and the appearance of a large number of carbon atoms with the sp^2-hybridisation of their orbitals.[10] For this reason, strictly speaking, the study of Iwaki *et al.*[7] dealt with the electrochemistry of non-diamond (amorphous) carbon and not with the diamond proper.

In fact, the electrochemistry of diamond was started with the study reported in Ref. 11. In this work, the $I-V$ characteristic was derived for the first time and the differential capacitance at the diamond/electrolyte solution interface was measured; photosensitivity of diamond electrodes was also revealed and related to the semiconductor properties of diamond. A few years later, these investigations of Russian researchers were followed by studies carried out by electrochemists in Japan, Israel, France, USA and other countries. For the last three years the number of publications devoted to diamond electrodes has increased dramatically.

This review generalises the most important results from studies of electrochemical properties of synthetic semiconductor diamond and application of electrochemical methods for the determination of characteristics of diamond films and outlines perspectives of the development of this new branch of electrochemistry.

Yu V Pleskov A N Frumkin Institute of Electrochemistry, Russian Academy of Sciences, Leninsky prosp. 31, 117071 Moscow, Russian Federation. Fax (7-095) 952 08 46. E-mail: pleskov@electrochem.msk.ru

Received 18 November 1998
Uspekhi Khimii **68** (5) 416 – 429 (1999); translated by V D Gorokhov

II. Preparation of diamond thin-film electrodes

Since the work reported in Ref. 11 until now the subjects of virtually all studies have been diamond films prepared by the method of chemical vapour deposition (CVD). The studies by Derjaguin *et al.*[12] carried out in the 1970s were an important stage in the development of this method. The CVD method relies on the deposition under subatmospheric pressure from an activated gas phase consisting of a volatile organic substance and hydrogen.[3, 13] The gas phase activation is required in order to create sufficiently high concentration of active carbon-containing species. These particles, by colliding against the surface of a heated substrate, disintegrate and release carbon atoms from which the crystalline lattice of diamond is formed. In the temperature and pressure ranges used, the diamond is metastable; the stable form is another allotropic carbon modification known as graphite. The gas phase activation should lead to the appearance of a reagent suppressing the deposition of non-diamond forms, *viz.*, graphite and amorphous carbon. Atomic hydrogen is such a reagent; in its atmosphere graphite 'burns out', while diamond remains unaltered.

Current practices rely basically on the use of thermal and electric (sometimes, chemical and photochemical) methods of gas activation. In the case of thermal activation, a reactor for vapour deposition of diamond films is used (Fig. 1). Above the substrate, on which diamond is supposed to grow, an activator is suspended in the form of wire made of a high-melting metal (W, Ta). This wire is heated to incandescence (~ 2000 °C) at which temperature the H_2 molecules dissociate at a sufficiently high rate. The gas phase is a mixture of carbon-containing gases (methane, acetone or methanol vapour, *etc.*, usually at concentrations of up to 5%) with hydrogen. Their contacts with the activator surface yield, along with the hydrogen atoms, excited carbon-containing molecules and radicals that are transferred towards the substrate surface, where deposition of diamond film takes place.

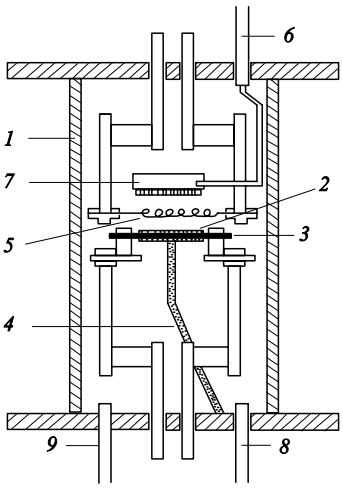


Figure 1. Scheme of a reactor for the chemical vapour deposition of diamond films under thermal activation;[3]
(*1*) reactor body; (*2*) substrate; (*3*) substrate heater; (*4*) thermocouple; (*5*) heated tungsten wire; (*6*) gas input; (*7*) diffuser; (*8*) pipe-line to a vacuum pump; (*9*) pipe-line to a manometer.

Electrical activation is induced using various forms of electric (arc, glow) discharge with the use of constant and alternating current (high frequency, ultra-high frequency, pulse mode). Each version of the electric method has its own advantages and disadvantages. For example, the electric arc discharge permits high deposition rates ranging from tens to hundreds of micrometers per hour. Under the ultra-high-frequency activation, the plasma ensures homogeneous conditions for the deposition over a large surface area of the substrate.

Depending on the aim of particular studies, the role of the substrate is played by metals (W, Mo), silicon (wafeas with a mirror-polished surface that are frequently used in microelectronics), glassy carbon, *etc.* Crystallisation is primed by diamond microcrystals seeded on the support surface. Later, the silicon substrate can be easily etched to obtain the so-called free-standing films. If the substrate is a diamond single crystal (natural or synthetic), then epitaxial growth takes place: the growing film repeats the crystalline structure of the substrate and forms a single crystal (such films are called homoepitaxial). Usually, the film thickness is a few micrometers, but in some cases it may reach several millimetres. The area covered with a diamond film reaches 10×10 cm and more, though the electrochemical studies usually use electrodes $\sim 1 \times 1$ cm in size.

As noted above, in order to make a diamond film electroconducting, one should dope it (usually in the process of its growth) with boron. For this purpose, the gas phase is supplemented with a volatile boron compound, *e.g.*, trimethyl borate, in the concentration ranging from 10 to 10 000 ppm. Alternatively, a solid source of boron is placed near the activator and the substrate. In the latter case, the boron is transferred into the gas phase as a result of the activation. It has been established empirically that the content of boron in the growing film is approximately proportional to its content in the gas phase.[14] The specific resistance of diamond depends on the content of boron in the film: it can vary, *e.g.*, from 10^4 Ohm cm (at a content of boron atoms in diamond of $\sim 10^{18}$ cm^{-3}) to tenth and even thousandth fractions of Ohm cm (at a content of boron atoms in diamond $\sim 10^{21}$ cm^{-3}). As its resistivity decreases, the dielectric diamond acquires successively the properties of a semiconductor, a degenerate semiconductor and then of a semimetal.

The energy of boron ionisation in diamond is great compared with the thermal energy (kT). At room temperature, the activation energy is 0.37 eV and decreases appreciably at high boron concentrations.[15] Hence, the concentration of the majority charge carriers (holes) is 2–3 orders of magnitude lower than that of the boron atoms (acceptors).

It should be pointed out that the methods of chemical and physical vapour deposition are widely used for the preparation of not only crystalline (diamond) films but also films of amorphous hydrogenated carbon a-C:H[10] in which there is no long-range ordering of the C–C bonds (hence, there is no crystalline structure), but the short-range ordering exists. Of a wide diversity of amorphous carbon films, one can conditionally distinguish graphite- and diamond-like films. Hybridisation of the carbon atom orbitals is predominantly of the sp^2-type in the former and of the sp^3-type in the latter. The graphite-like films are characterised by a small width (< 1 eV) of the gap and have high electric conductivity. The diamond-like films have a wider (2–4 eV) gap and are appreciably less conductive; certain properties of these films are similar to those of diamond (and this explains their name).

In addition to thin films, individual diamond crystals grown at high temperature and high pressure can also be used as electrodes. Such crystals are obtained from a carbon solution in molten metals (*e.g.*, Ni–Fe–Mn) in the pressure and temperature ranges corresponding to the region of thermodynamic stability of diamond; diamond crystals are doped with boron during their growth.

III. Crystal structure and basic electrophysical characteristics of diamond films

1. Crystal structure

Polycrystalline films consist of crystallites the size of which increases with the film growth approximately proportionally to its thickness and reaches a few micrometers. Facets of crystallites usually form a characteristic faceted morphology of the film surface.

The perfection of the crystalline structure of deposited films is monitored by recording their Raman spectra. A typical spectrum of a diamond film is shown in Fig. 2. The crystalline diamond is characterised by a narrow peak at 1332 cm^{-1} due to the first-order scattering on the crystal lattice. Two blurred bands at $\sim$ 1350 and $\sim$ 1550 cm^{-1} correspond to the non-diamond carbon form with the predominant sp^2-hybridisation. When comparing the diamond peak and the maximum determined by the sp^2-carbon in the spectrum, one should bear in mind that the magnitude of Raman signal on the ordinate (Fig. 2) is 50 times more sensitive to the non-diamond carbon form than to the crystalline diamond.[16] In the best specimens employed as electrodes, the admixture of the non-diamond form did not exceed 1% (as confirmed by independent electrochemical measurements). According to Hashimoto *et al.*,[17] the admixture content decreases in the film substrate surface direction. Nevertheless, modern physical techniques (Raman and Auger spectroscopy, atomic-force microscopy) do not provide sufficiently exhaustive characterisation of non-diamond carbon inclusions in polycrystalline diamond films. It is by electrochemical measurements that these inclusions are revealed.[18]

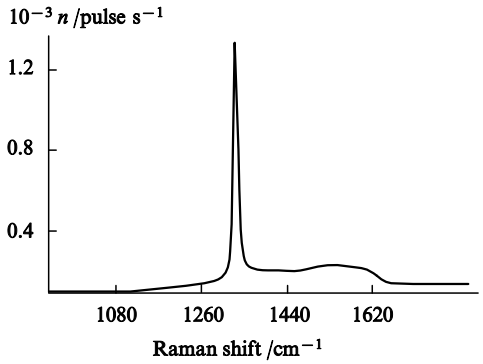


Figure 2. Raman spectrum of a polycrystalline diamond film.

In polycrystalline diamond films, the non-diamond form is represented primarily by a disordered carbon of intercrystallite boundaries, the outcrops of which on the diamond surface were observed using high-resolution electron microscopy.[19] The thickness of the intercrystallite boundaries in diamond films reaches a few nanometers. In addition, the crystal lattice of films has various defects. In some instances, a thin (about several nanometers) non-diamond layer coating the diamond film was revealed. This layer is often formed in the latest (poorly controlled) stages of film growth after cessation of the gaseous phase activation. To remove it, samples are heated in air to 520 °C or boiled in concentrated $HClO_4$, dichromate-sulfuric acid mixture or solutions of other strong oxidants. Such a treatment of the non-diamond carbon form results in its oxidation to CO_2.

2. Electroconductivity of films

Specific resistance of diamond films is determined not only by the concentration but also by the mobility of free charge carriers. Usually, the mobility of the holes in polycrystalline films is not high; it is lower than that in natural single crystals (usually, of the magnitude of 1 $cm^2\ V^{-1}\ s^{-1}$),[20–22] although in some cases it reaches tens and hundreds of $cm^2\ V^{-1}\ s^{-1}$ (see, *e.g.*, Refs 23 and 24). The mobility of the holes in single-crystal (homoepitaxial) films is 1–2 orders of magnitude higher than that in polycrystalline films grown under the same conditions.[22] In films of amorphous diamond-like carbon, the mobility is several orders of magnitude lower than that in crystalline diamond.[20]

The character of conductivity of doped polycrystalline films and its relation to the crystal structure were studied by the method of impedance spectroscopy.[25] The results obtained have made it possible to describe a conducting polycrystalline film using a simple model of a heterogeneous medium. According to this model, the medium consists of regularly distributed well-conducting crystallites of the same size separated by poorly conducting intercrystallite boundaries, which form a continuous matrix. Undoubtedly, such a model simplifies the structure of a real film in which crystallites are distributed over its thickness with regard to their size, while individual acicular crystallites penetrate through the entire film thickness. Nevertheless, this model is applicable in the studies of moderately doped diamond films. The theory of complex conductivity of a heterogeneous medium [26] developed for the model described has made it possible to determine the bulk proportion of the boundary phase in the film ($\sim$ 5%, which in order of magnitude correlates with the above-mentioned results of Raman spectroscopy) and to estimate conductivities of crystallites † and intercrystallite boundaries as 10^{-4} and 10^{-7} $Ohm^{-1}\ cm^{-1}$, respectively.

Similar conclusions about the character of conductivity of polycrystalline films were made by Sokolina *et al.*[27] Subsequent studies devoted to thorough investigation of the frequency dependence of the impedance of polycrystalline films [28–30] have shown that at high temperatures the electric conductivity due to the motion of free holes in the valence band should be supplemented with a component determined by the jump-over of holes between localised traps (possibly, associated with the intercrystallite boundaries).

IV. Synthetic diamond films as electrodes: resistance to corrosion and background current – potential curves

In the assessment of novel electrode materials used in electrolysis, electroanalysis and manufacture of electrochemical sensors and other devices, the main attention is paid to the magnitude of background current and the width of the potential range in which this current remains sufficiently low and does not interfere with measurements as well as to the corrosion resistance and stability of materials. The diamond electrode meets all of these criteria.

Let us consider the current-potential curves in solutions of indifferent electrolytes as the initial characteristic of the electrode behaviour of diamond.[31–33] It is these curves that form the 'background' against which the kinetic, impedance, photoelectrochemical and electroanalytical characteristics of diamond electrodes are manifested.

An advantage of diamond electrodes is a wide potential range of weak background currents, which is sometimes called the range of ideal polarisability. It is obvious in comparison with other materials, which are widely used as electrodes (platinum, glassy carbon, graphite, *etc.*).

Figure 3 shows characteristic polarisation curves recorded using a solution of an indifferent electrolyte (0.5 M H_2SO_4) in the potentiodynamic mode of potential cycling on the polycrystalline diamond thin-film electrodes and the electrodes from platinum and highly oriented pyrographite which are traditionally applied in electrochemistry.

According to Martin *et al.*,[32] all the diamond films used as electrodes may be divided into 'good' and 'bad' films, depending on the width of the ideal polarisability range. For the 'good' films, this range reaches $\sim$ 3 V at the current density j of several mA cm^{-2} and at least about 1.5 V for the j values making up a few decimal fractions of 1 μA cm^{-2} (Fig. 3*a*). For the 'bad' films, the range of ideal polarisability is appreciably narrower (Fig. 3*b*); there is a noticeable hysteresis, which naturally restricts their

† In the studies reported in Refs 11 and 25, the conductivity of diamond films was associated not with the boron incorporation but rather with the presence of unidentified admixtures and/or defects due to specific conditions of deposition (in particular, an elevated temperature of the substrate).

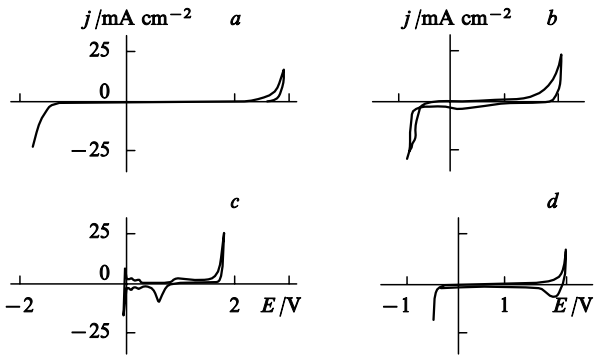


Figure 3. Polarisation curves of the electrodes made of polycrystalline diamond (*a*, *b*), platinum (*c*) and highly oriented pyrographite (basal plane) (*d*) in 0.5 M H_2SO_4;[33]
(*a*) 'good' film; (*b*) 'bad' film; potential was measured relative to the normal hydrogen electrode (NHE).

applicability as electrodes. Martin *et al.*[32] did not give any accurate definition of 'good' films but indicated that they were obtained at a low content ($\sim 1\%$) of a carbon-containing gas (methane) in the reaction system (the 'bad' films are formed at a methane content of $\sim 4\%$).

Comparison of the background currents for diamond and glassy carbon has shown that this current is 10 times as low on diamond.[34]

As regards its resistance to corrosion in aggressive media and under extreme potentials, the diamond demonstrates it in full measure. Multiple cycles of potential variation on the diamond electrode from the potential of hydrogen evolution on the cathode to the potential of oxygen evolution on the anode in the aggressive solution 1 M HNO_3 + 0.1 M HF had no effect on either the surface morphology of diamond (according to electron microscopy data) or the ratio of diamond and non-diamond carbon forms on the electrode surface (according to Raman spectra). Under the same conditions, the electrodes from glassy carbon and pyrographite underwent strong degradation.[35] A similar study was conducted in the solution 1 M HNO_3 + 0.1 M NaCl under the potentials of the chlorine evolution on the anode.[36] But in this case too, X-ray photoelectron spectroscopy showed that neither the morphology of the diamond surface nor the content of admixtures on it were altered.

On the other hand, prolonged 'cycling' of the diamond electrode potential in concentrated (15%) KOH solution can lead to corrosive degradation of the diamond surface. The extent and character of this degradation depend on the conditions of diamond growth, although this dependence has not been clearly established. The intercrystallite boundaries composed of the non-diamond carbon undergo the strongest degradation.[37]

In some cases (probably, in the presence of latent flaws in the film), prolonged polarisation of the diamond electrode in solution leads to the appearance in it of pinholes through which the electrolyte penetrates to the substrate.[38–40] On the electrode surface, some inactive sites may appear [41] as the result of local detachment of diamond films from the substrate or possibly because of a non-uniform doping of diamond with boron. The well-prepared films prove to be not only resistant to corrosion themselves but also to protect the metal substrate.[39, 42, 43]

If a diamond film was obtained in a hydrogen atmosphere, its surface is covered by a hydrogen monolayer and displays hydrophobic properties. This type of surface is also obtained after treatment of diamond in a hydrogen plasma.[44] On the contrary, an oxidised diamond surface contains the hydroxy groups and hence is hydrophilic.[32, 45] These two types of surface can also be obtained by electrochemical treatment consisting, respectively, in the cathodic or anodic polarisation in an aqueous electrolyte solution.[46]

In conclusion, let us consider properties of the electrodes made of diamond-like carbon. Here, the data are scarce and are somewhat contradictory. For example, Howe [47] has reported that even thin films (50-nm thick) are well resistant to corrosion, while Sakharova *et al.*[48, 49] have pointed out that such films proved to be permeable to the electrolyte, which by penetrating to the metal substrate resulted in its corrosion and led eventually to the film peeling. Films from diamond-like carbon of submicron thickness were found to be more resistant. Their background current – potential curves resemble analogous curves for the diamond electrode (Fig. 3*a*,*b*) but have a narrower range of ideal polarisability.[50]

V. Impedance spectroscopy and semiconductor properties of diamond electrodes

1. Linear impedance. Equivalent circuits

Measurement of frequency characteristics of electrochemical systems makes it possible to derive information on their microscopic structure, as well as on the nature and kinetics of the charge transfer processes that occur in them. Linear impedance can be measured if a harmonic electrical signal with the frequency f is applied to the cell and then the real ($\mathrm{Re}Z$) and imaginary ($\mathrm{Im}Z$) components of the impedance Z are determined by analysing the spectrum of the system response with an appropriate device.

In studies of the impedance of diamond electrodes, the greatest attention is paid to the following peculiarities: the semiconductor character of diamond (for moderately doped films) and a special type of the frequency dependence of the impedance characteristic of the overwhelming majority of films.

In its general form, the impedance of a thin-film electrode may be represented by the three equivalent circuits shown in Fig. 4. The circuit depicted in Fig. 4*a* includes two *RC*-chains, one of which belongs to the diamond film itself and the other relates to the diamond/electrolyte solution interface. In the first chain, R_s is the ohmic resistance of the diamond film and C_g is the geometrical capacitance of the film; in the second chain, C_{sc} is the differential capacitance of the space charge region at the diamond/solution interface and R_F is the differential resistance to the process of charge transfer at this interface (the so-called Faraday resistance).

The geometrical capacitance of most films is low (of the order of 10^{-9} F cm^{-2}); as regards the order of magnitude, the corresponding impedance is larger than the film resistance R_s (except for very lightly doped films), and hence the latter may be neglected. In this case, we obtain a simple equivalent circuit with three elements (Fig. 4*b*) which is known as the Randles – Ershler circuit.[51] It is essential that all the elements of the above circuits are independent of signal frequency. The circuit represented by Fig. 4*c* includes a frequency-dependent, constant phase-shift element (CPE) (see below).

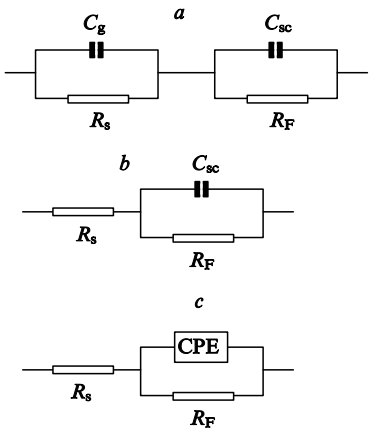


Figure 4. Equivalent circuits of the impedance (see text).

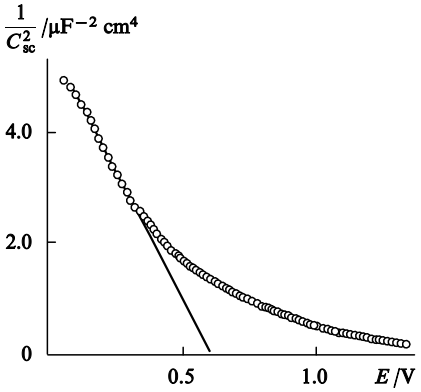


Figure 5. The Mott–Schottky plot for a boron-doped polycrystalline electrode with frequency-independent capacitance in 0.5 M H_2SO_4.[52]

In certain cases, the impedance spectra of diamond electrodes are well described by the equivalent circuit (Fig. 4*b*) with a virtually frequency-independent (in the range of $1-10^5$ Hz) capacitance.[52] Figure 5 presents the Mott–Schottky plot, which expresses the dependence of the squared reciprocal capacitance C_{sc} on the polycrystalline diamond electrode potential E in 0.5 M H_2SO_4. Physically, it reflects the dependence of the space charge layer thickness in a semiconductor on potential.[6] The space charge arises because the near-surface region of semiconductors is depleted in mobile charge carriers (the so-called depletion layer). Extrapolation of the linear segment until its intersection with the abscissa provides the value of flat-band potential of the electrode E_{fb}, while the slope of this line can be used for calculating the concentration of non-compensated acceptors in a semiconductor by the formula

$$N_a = -\frac{2}{e\varepsilon_0\varepsilon}\left[\frac{d(C_{sc}^{-2})}{dE}\right]^{-1}, \quad (1)$$

where e is the electron charge, ε and ε_0 are the dielectric constants of diamond and vacuum, respectively. Formula (1) was derived under assumptions that, first, the potential drop during polarisation takes place in the space charge region (and, *e.g.*, not in the Helmholtz layer at the interface); second, there is no ionisation of 'deep' acceptors; third, the measured capacitance is that of the space charge region C_{sc} (and does not include, *e.g.*, the capacitance of surface states, adsorption capacitance, *etc.*). For the electrode under discussion (see Fig. 5), $N_a \simeq 3.1\times10^{18}$ cm^{-3}.

The depletion layer is usually formed in a doped wide-bandgap semiconductor which is in contact with another phase (metal, electrolyte solution or vacuum). The potential barrier associated with the depletion layer formation (in particular, upon contact with the conducting phase) is called the Schottky barrier. The contact of polycrystalline diamond films with certain metals (Au, Pt, Pd) manifests a rectifying effect (see, *e.g.*, Refs 53 and 54), while its capacitance characteristics resemble those of the diamond/indifferent electrolyte contact.

However, specimens with a frequency-independent capacitance represent an exception rather than the rule. Usually, the capacitance of diamond films depends on frequency. Figure 6 features a characteristic electrode impedance spectrum presentation on a complex plane.[55] At high frequencies (1–100 kHz), the complex-plane plot forms a straight line that does not pass through the origin of coordinates (see Fig. 6*a*). A similar impedance feature was observed in a series of studies (see, *e.g.*, Refs 56–59). At low frequencies, the $-\mathrm{Im}Z$ *vs.* $\mathrm{Re}Z$ plot is curved due to the presence of the Faraday resistance in the equivalent circuit (Fig. 6). Under the anodic or cathodic polarisation, the curvature becomes more appreciable due to the decrease in R_F, and the shape of the low-frequency segment of the curve approaches a semicircle.

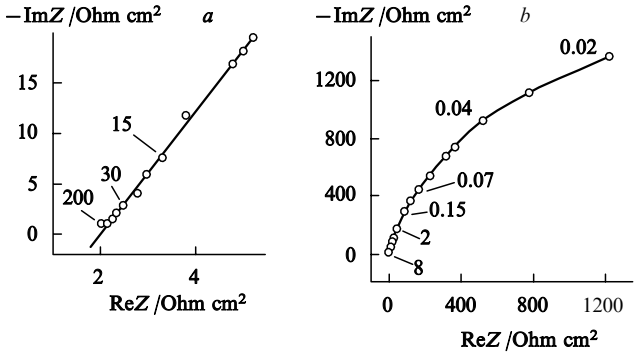


Figure 6. High-frequency (*a*) and low-frequency (*b*) segments of the complex-plane plot of the impedance of a single-crystal electrode in 0.5 M H_2SO_4 under a steady-state potential.[35] Numerals at the curves indicate the signal frequencies /kHz.

Such a characteristic type of the frequency dependence suggests that the equivalent circuit of the electrode includes the so-called constant phase element (CPE) with its impedance equal to

$$Z_{CPE} = \sigma^{-1}(i\omega)^{-a}, \quad (2)$$

where the frequency-independent parameter σ has the dimensionality F^a Ohm^{a-1} cm^{-2}, the index a determines the character of the frequency dependence, i is the imaginary unity, $\omega = 2\pi f$ is the angular frequency of the alternating current. Analysis of the impedance spectra is based on the equivalent circuit (Fig. 4*c*) derived from the Randles–Ershler circuit by replacing the frequency-independent capacitance with CPE. The elements of the equivalent circuit are usually calculated by the least-squares method with minimisation of the standard deviation of the logarithm of the impedance modulus measured at different frequencies from the logarithm of the impedance modulus calculated for the equivalent circuit using the corresponding computer programme.[60]

Typical σ and a values, film resistance R_s, calculated diamond resistivity ρ and the Faraday resistance R_F are listed in Table 1 for the polycrystalline and single-crystal (thin-film and compact) diamond electrodes and the electrode made of amorphous diamond-like carbon.[50,61] Comparison of the data presented in

Table 1. Parameters a, R_s (Ohm cm^2), σ (μF^a Ohm^{a-1} cm^{-2}), ρ (Ohm cm) and R_F (Ohm cm^2) found in the studies of the impedance of polycrystalline and single-crystal diamond films in 0.5 M H_2SO_4 solution.

Electrode	Substrate	Film thickness /μm	a	R_s	σ	ρ	R_F
Polycrystalline film	W	2.4	0.92	1.5	1–1.5	0.7×10^4	10^4-10^7
Single-crystal film	synthetic diamond single crystal	10	0.96	32	2.7	0.1	10^6-10^8
Single crystal[a]	–	–	0.92	2.8	2.5	30	10^6
Amorphous diamond-like film	glassy carbon	0.07	0.9	–	0.05	0.8×10^5	10^6

[a] A single crystal grown under high pressure and high temperature.

Table 1 suggests that in both the qualitative respect (the equivalent circuit form and the presence of CPE in it) and the quantitative respect (typical a and σ values) the polycrystalline and single-crystal electrodes are virtually the same: a varies within a narrow range 0.9–0.96, $\sigma \simeq 1-3$ μF^{a-1} Ohm^{a-1} cm^{-2}, $R_F \approx 10^4-10^8$ Ohm cm^2 (in an indifferent electrolyte solution under a stationary potential). Assuming that the measured integral impedance parameters a and σ characterise the double electrical layer on diamond electrodes, it may be concluded that the structure of this layer is approximately the same in the polycrystalline and single-crystal specimens. Furthermore, on the whole, the structure of the double electrical layer is identical in the diamond and wide-bandgap diamond-like carbon electrodes.

Rather high values of the Faraday resistance R_F reflect the above-mentioned low background currents and the negligibly small corrosion of diamond in aqueous solutions. Larger values of σ in comparison with those in other semiconductor electrodes are indicative of a relatively high doping level of the diamond films studied (the acceptor concentration $N_a \geqslant 10^{18}$ cm^{-3}).

Note that according to different authors, the flat-band potential (E_{fb}) values determined by the extrapolation of the Mott–Schottky plots are in the range from 0.5 V (Ref. 52) to 1.2 V (Ref. 55) [relative to the saturated calomel electrode (SCE)]. Such a spread of data can in part be explained by different degrees of diamond surface oxidation (resulting from pretreatment of samples). It is known[6] that the anodic and cathodic oxidation of numerous semiconductors shifts their flat-band potentials toward positive and negative regions, respectively. This is largely due to an appreciable extent to the dipolar potential drop associated with the oxygen monolayer adsorbed on the electrode surface and determined by the polarity of the C–O bonds.

Note in conclusion that in the CPE-containing equivalent circuit of the electrode, no separate frequency-independent capacitance was revealed that could be attributed to the space charge region in diamond.[62] This means that it is the CPE [with its dependence on potential which is characteristic of semiconductor electrodes (see Section V.2 for more detail)] that describes the properties of the space charge region.[62]

Recently, the diamond crystals grown under high pressure and high temperature have been used for the first time as electrodes. Their impedance characteristics proved to be close to those of thin-film electrodes (see Table 1).[63, 64]

2. On the nature of the frequency dependence of the differential capacitance of diamond electrodes

Naturally, the dependence of capacitance on frequency that follows from the impedance complex-plane plot (see Fig. 6) determines the slope of the straight line in the Mott–Schottky plot.[65] The researchers investigating the frequency dependence of the differential capacitance of diamond electrodes must answer two major questions, *viz.*, what processes lead to the appearance of this dependence and what is the most convenient manner of its formal presentation.

The nature of the frequency dependence of the slope of the Mott–Schottky plot for the semiconductor electrodes has been subject to discussion for over three decades (see, *e.g.*, Refs 6 and 66). Possible reasons for its appearance are believed to be the dependence of dielectric relaxation on frequency in the space charge region,[67] roughness of the electrode surface,[66] slow ionisation of deep donors (acceptors) in the space charge region of semiconductors[68] and the influence of the surface states.

Evstefeeva *et al.*[69] investigated the dependence of capacitance on frequency in its application to the diamond electrode assuming that the electrode surface roughness should not necessarily lead to the appearance of CPE in its impedance.[70] The hypothesis [59] of slow ionisation of atoms with a deep-lying energy level (*e.g.*, boron) in the space charge region of diamond crystals has been assumed for a tentative explanation of the frequency dispersion of the Mott–Schottky plots of diamond electrodes. This explanation is supported by the fact that the magnitude of σ varies regularly with changes in the thickness of the space charge layer (in conformity with Schottky's theory), whereas the magnitude of a is virtually independent of both the potential and the solution dilution, *i.e.*, the factors influencing the electrode surface state. Therefore, it has been concluded that the observed dependence of capacitance on frequency is not associated with the surface states but is determined by the process occurring in the space-charge region of diamond.‡

Let us consider different forms of the Mott–Schottky plots when they are frequency-dependent using the diamond electrode as an example. As noted above, this situation is typical of the electrochemistry of various semiconductor electrodes. Figures 7 and 8 illustrate three ways of presentation of such plots. The first pattern is a 'sheaf' of $C^{-2}-E$ straight lines plotted from the capacitance values measured directly at a given frequency (a series of frequencies) and potential (see Fig. 7). The second one is the plot $C_{calc}^{-2}-E$ (see Fig. 8, curve *2*). When plotting this curve, the real equivalent electrode circuit (see Fig. 4*c*) was replaced by a simpler circuit (see Fig. 4*b*) including the frequency-independent capacitance instead of CPE. In its essence, the C_{calc} is the capacitance C_{sc} averaged over the entire range of the alternating current frequencies studied. As this step uses the body of experimental data for the whole frequency range, the value of C_{calc} obtained may be regarded formally as the frequency-independent one. Finally, the third pattern (for the cases where the equivalent circuit contains CPE) is the $\sigma^{-2}-E$ plot (see Fig. 8, curve *1*). Note that $\sigma \to C_{calc}$ at $a \to 1$.

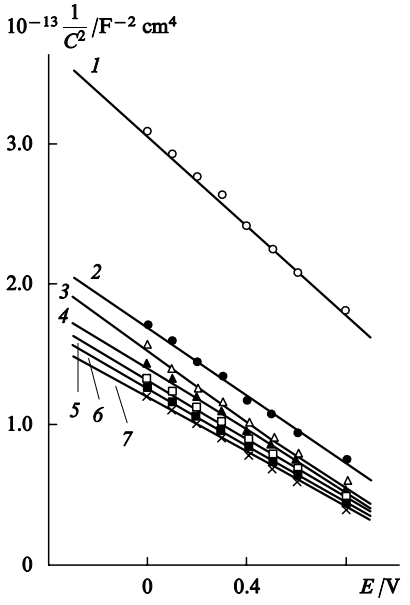


Figure 7. The Mott–Schottky plot for a boron-doped single-crystal electrode with a frequency-dependent capacitance in 0.5 M H_2SO_4. Frequency/Hz: (*1*) 21 544; (*2*) 10 000; (*4*) 4642; (*5*) 2154; (*6*) 1000; (*7*) 215; (*3*) the curve is calculated for C_{calc};[69] the potential values were measured relative to the Ag/AgCl electrode.

When comparing the above-listed patterns, one should pay attention to the fact that the plot σ^{-2} *vs.* E is frequency-independent, since σ is the frequency-independent parameter by definition [see formula (2)]. It may be considered as the most general case and be used for comparing results of different experiments, since in this case the contribution from the intrinsic frequency-dependent element is ruled out. However, taking into

‡ It is unclear until now why the differential capacitance of some diamond electrodes is independent of frequency.

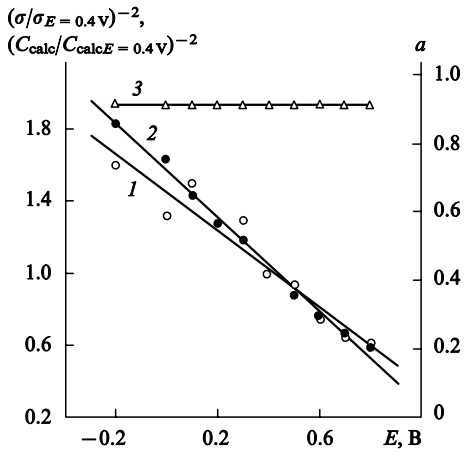


Figure 8. Dependence of $(\sigma/\sigma_{E=0.4\ V})^{-2}$ (*1*), $(C_{calc}/C_{calc_{E=0.4\ V}})^{-2}$ (*2*) and *a* (*3*) on potential for a single-crystal electrode (calculated using the data of Fig. 7).[69] Potentials were measured relative to the Ag/AgCl electrode.

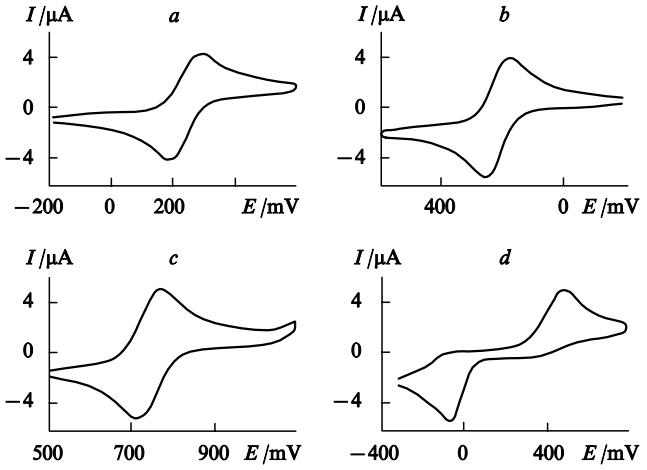


Figure 9. Cyclic voltammograms in 10^{-4} M solutions of $Fe(CN)_6^{3-/4-}$ (*a*), $Ru(NH_3)_6^{2+/3+}$ (*b*), $IrCl_6^{2-/3-}$ (*c*) against the background of 0.1 M KCl and quinone/hydroquinone (*d*) against the background of 0.1 M $HClO_4$.[73] Potentials were measured relative to the SCE.

account the dimensionality of σ, correct comparison of the calculated data with the published results of direct capacitance measurement on diamond electrodes seems questionable.

The use of the $C_{calc}^{-2} - E$ dependence removes the dimensionality problems, although a somewhat formal character of the C_{calc} parameter is a disadvantage of this form of the Mott–Schottky plot presentation.

The sheaf of $C^{-2} - E$ straight lines may be interpreted as manifestation of a slow process (*e.g.*, the above-mentioned ionisation of the deep acceptor) occurring in the space charge region of a semiconductor. Unfortunately, the nature of the dependence of differential capacitance on frequency is unknown; therefore, one should consider as approximate the literature data on the concentration of acceptors in diamond calculated on the basis of Schottky's theory for an arbitrary frequency of the measured signal. Nonetheless, it appears more convenient to use the dependence $\sigma^{-2} - E$ (especially for the cases when the exponent *a* is close to 1) or $C_{calc}^{-2} - E$ for qualitative comparison of electrodes made of the same semiconductor material.

VI. Kinetics of the electrode reactions

1. Kinetics of outer-sphere reactions. Metal-like diamond electrodes

It is common practice to divide electrochemical reactions into outer-sphere (occurring without cleavage of interatomic bonds in the reacting molecule) and inner-sphere ones (occurring with the cleavage or formation of such bonds). An example of outer-sphere reactions is the electron transfer in the $Fe(CN)_6^{3-/4-}$ system, while the inner-sphere reactions may be exemplified by the oxidation and reduction of water molecules with the evolution of O_2 and H_2, respectively. Let us start discussion of the kinetics of reactions on the diamond electrode with the former type of reactions.

A number of outer-sphere reactions were investigated by the method of potentiodynamic curves with a linear potential sweep. This method proved to be convenient for both qualitative and quantitative characterisation of the electrode behaviour. The theory of this method has been considered in textbooks.[71, 72]

Typical cyclic voltammograms recorded for four redox systems are presented in Fig. 9. The outer-sphere reactions occur in solutions of $Fe(CN)_6^{3-/4-}$, $Ru(NH_3)_6^{2+/3+}$ and $IrCl_6^{2-/3-}$, while the inner-sphere raction occurs in the quinone/hydroquinone system. A characteristic shape of all curves with peaks of anodic and cathodic currents demonstrates that in all cases the stage of charge transfer at the interface is rather fast; the reaction is hampered due to the insufficiently rapid reagent mass transfer in solution toward the electrode surface. Similar curves were obtained in a series of studies of the ferrocyanide/ferricyanide[74] and quinone/hydroquinone systems,[75] Ce^{3+} ions (see Ref. 76), *etc.*

Analysis of these curves makes it possible to determine the following characteristics of the diffusion and interphase charge transfer: diffusion coefficient, transfer coefficients of the cathodic (α) and anodic (β) reactions and the rate constant (k^0). Quantitatively, the larger the difference between the potentials of the cathodic and anodic peaks the less reversible the electrode reaction. According to the theory of electrode kinetics,[71, 72] for a reversible one-electron reaction at room temperature, $\Delta E_p = 56$ mV irrespective of the reagent concentration and the rate of potential sweep. For the systems, the voltammograms of which are shown in Fig. 9*a*–*c*, the values of ΔE_p are 88, 72 and 65 mV, respectively.[73] Consequently, on a relatively strongly doped polycrystalline electrode, the processes under consideration occur in the mode of a quasi-reversible reaction. On the contrary, the electrode reaction is markedly irreversible in the quinone/hydroquinone system: $\Delta E_p = 560$ mV. These qualitative estimates correlate with the values of rate constants determined for the above-listed redox systems.[77]

Reagent	$Fe(CN)_6^{3-/4-}$	$Ru(NH_3)_6^{2+/3+}$	$IrCl_6^{2-/3-}$	quinone/hydroquinone
k^0 /cm s^{-1}	9×10^{-4}	3×10^{-3}	4×10^{-3}	$< 10^{-6}$

The rate constants strongly depend on both the level of diamond doping with boron (see below) and the prior preparation of the electrode surface; these data are presented here for the purpose of illustration. On the whole, based on the studies of a series of systems [including methyl viologen; $FeL_3(ClO_4)_2$, where L is *o*-phenanthroline; 1,1′-dimethoxyferrocene, *etc.*], the following qualitative inferences have been made:[78, 79] the outer-sphere reactions are closer to reversible reactions that the inner-sphere ones; the reactions in the systems with a positive equilibrium potential are closer to reversible reactions than those in the systems with a negative potential;§ on the heavily doped metal-like diamond the reaction rate is higher than on the moderately doped electrodes characterised by semiconductor properties. But even on the metal-like diamond electrodes the reaction rate is appreciably lower than that on the metal electrodes with high electrocatalytic activity, *e.g.*, platinum. Consequently, upgrading

§ This regularity is invalid for the $Ce^{3+/4+}$ system (see Ref. 75) which is discussed in more detail in the next section.

of electrocatalytic properties of diamond electrodes intended for practical applications is a topical problem. First experiments have shown [80, 81] that the deposition of microquantities of platinum onto the diamond electrode surface reduces the overvoltage of the cathode reactions.

2. Semiconductor properties of diamond and the electrode kinetics

The systems $Fe(CN)_6^{3-/4-}$, quinone/hydroquinone ¶ and $Ce^{3+/4+}$ have been investigated quantitatively.[75, 80, 82] The dependences of the potentials of the anodic and cathodic current peaks E_p in the potentiodynamic curves on the logarithm of the rate of potential sweep υ were determined experimentally; the data characterising the quinone/hydroquinone system are shown in Fig. 10.[75] The transfer coefficients of the anode and cathode reactions were calculated from the slope of the straight line (Fig. 10 *c*) using the theory of the method of potentiodynamic curves.[72]

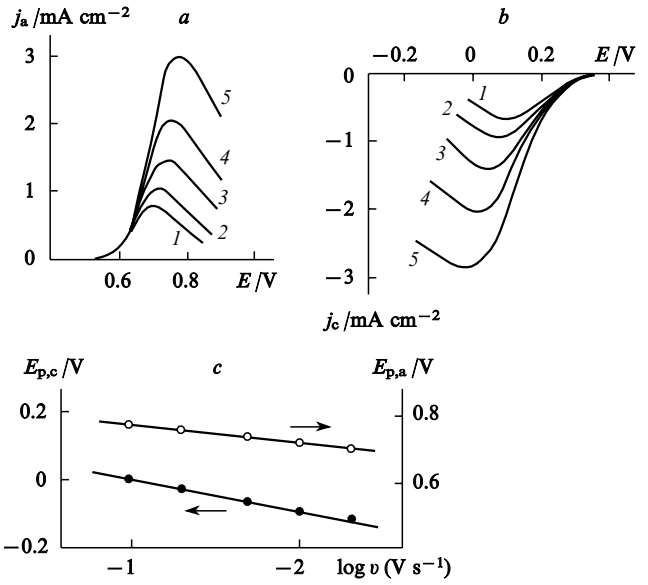


Figure 10. Potentiodynamic curves recorded during the linear potential sweep in the course of hydroquinone (0.01 M) oxidation (*a*) and quinone (0.01 M) reduction (*b*) in 0.5 M H_2SO_4 on a polycrystalline diamond electrode, and dependences of the potentials of the cathodic ($E_{p,c}$) and anodic ($E_{p,a}$) current peaks on the logarithm of the sweep rate (*c*).[75] The rate of potential sweep /V s^{-1}: (*1*) 0.005; (*2*) 0.01; (*3*) 0.02; (*4*) 0.05; (*5*) 0.1. Potentials were measured relative to the Ag/AgCl electrode.

Table 2 presents the measured α and β values typical of the single-crystal and polycrystalline thin-film electrodes and a single crystal (grown under high pressure and high temperature) in Ce^{3+} and Ce^{4+} solutions. For the $Ce^{3+/4+}$ system (as for the two other systems, *viz.*, $Fe(CN)_6^{3-/4-}$ and quinone/hydroquinone), the transfer coefficients are less than 0.5, especially for the cathodic reaction, and the sum $\alpha + \beta$ proves to be less than unity. According to the theory of the electrochemical kinetics on semiconductors,[6] in the case of an 'ideal' *p*-type semiconductor electrode, the transfer coefficients for the reactions occurring with the participation of holes should be as follows: $\alpha = 0$, $\beta = 1$; $\alpha + \beta = 1$. In practice, however, the ideal case is extremely rare even for single-crystal semiconductor materials (silicon, gallium arsenide, *etc.*) that are prepared using much more advanced technologies than the technology for the preparation of polycrystalline CVD-diamond. The reason for the deviation from 'the ideal situation'

¶ Note that the reactions occurring in the quinone/hydroquinone system are inner-sphere ones.

Table 2. Kinetic characteristics of diamond electrodes in a 0.01 M Ce^{3+} (or Ce^{4+}) + 0.5 M H_2SO_4 solution.

Electrode	α	β	k^0 /cm s^{-1}
Polycrystalline film [55]	0.16	0.46	6×10^{-9}
Single-crystal film [55]	0.2	0.43	6.5×10^{-7}
Single crystal grown under high pressure and high temperature [63]	0.33	0.27	4.4×10^{-6}

appears to lie in the fact that during the electrode polarisation, part of the interphase potential drop is lost in the Helmholtz layer (*e.g.*, due to a high density of the surface states). As a result, the transfer coefficients α and β have the values intermediate between those characteristic of semiconductors (0 or 1) and metals (~ 0.5).

Extrapolation of the impedance complex-plane plot until its intersection with the Re*Z* axis (Fig 6*a*) gives the diamond film resistance R_s from which the diamond resistivity ρ can be calculated. The dependences of R_F on ρ for two redox systems are presented in Fig. 11. It is seen that, first, the reaction rate in the $Fe(CN)_6^{3-/4-}$ system is approximately three orders of magnitude higher than that in the quinone/hydroquinone system, which is consistent with the above-cited rate constants; second, R_F is observed to be directly proportional to ρ over a wide range of diamond resistivity. The existence of such a dependence for diamond electrodes was first reported by Modestov *et al.*[80] It reflects the fundamental law of the kinetics of reactions on semiconductor electrodes: the rate of an electrochemical reaction is proportional to the concentration of free carriers on the electrode surface. Indeed, the concentration of holes in the diamond bulk p_0 is inversely proportional to its resistivity ρ.† The concentration of holes on the electrode surface p_s is related to p_0 by the Boltzmann equation [6]

$$p_s = p_0 \exp\left(-\frac{e\phi_{sc}}{kT}\right),$$

where ϕ_{sc} is the potential drop in the space charge layer.

If the chemical interaction of diamond with the solution and hence the potential distribution over the diamond/solution interface is assumed to be independent of the level of diamond doping with boron, then at the given electrode potential which is set by the redox system the value of $e\phi_{sc}$ is the same for all electrodes. Consequently, the reaction rate ($\sim 1/R_F$) should be proportional

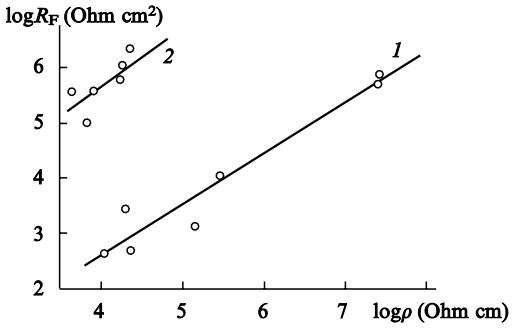


Figure 11. Dependence of the Faraday resistance under equilibrium potential in the $Fe(CN)_6^{3-/4-}$ (*1*) and quinone/hydroquinone (*2*) systems on the film resistivity.[83]

† In the discussion of the relation between the concentration of holes in specimens and their resistivity, it is assumed that the mobility of holes is independent of the boron concentration in specimens.

to the diamond conductivity, which is in fact observed in experiments.

3. Crystal structure and the electrode kinetics: comparison of electrodes from single-crystal and polycrystalline diamond and amorphous carbon

Polycrystalline diamond films are heterogeneous systems consisting of diamond crystallites and disordered carbon of intercrystallite boundaries (see Section III. 1). In this context, the following question arises: to what extent do the intercrystallite boundaries influence the electrochemical properties of polycrystalline diamond electrodes? In order to answer this question, one should compare the electrochemical behaviour of crystalline diamond with that of diamond-like carbon, which may be arbitrarily regarded as a model for the material of intercrystallite boundaries in the polycrystalline diamond.

Such a comparison shows that the kinetic characteristics (α and β) of single-crystal and polycrystalline diamond electrodes are similar. In solutions of redox systems, both types of diamond electrodes possess electrocatalytic activity (though not very great, which is characteristic of semiconductor electrodes).

The properties of amorphous carbon vary within very wide limits. In their electrode properties, the 'graphite-like' thin-film electrodes resemble conventional carbonaceous materials (*e.g.*, glassy carbon); redox reactions occur on them at high rates. On the contrary, in the case of 'diamond-like' electrodes there are no peaks of oxidation and reduction currents in such systems as $Ce^{3+/4+}$, $Fe(CN)_6^{3-/4-}$ and quinone/hydroquinone; the currents measured do not differ from the background current. The fact that the diamond-like carbon proved to be electrochemically inactive suggests that the intercrystallite boundaries make no practical contribution to the electrode behaviour of polycrystalline diamond; it is totally determined by diamond crystallites. This conclusion relies on the results of comparison of the impedance (Table 1) and kinetic (Table 2) characteristics of polycrystalline and single-crystal diamond films and seems to be valid at least in the range of moderate electrode polarisation.[55]

On the other hand, at high anode potentials (+1.7 V relative to the NHE, just before the beginning of oxygen evolution) a small peak is observed in the polarisation curve of a polycrystalline electrode in an indifferent electrolyte solution (similar to that shown in Fig. 3*a*).[32] Its height is as small as ~ 1 μA cm^{-2}; therefore, it can hardly be seen in Fig. 3*a* (and other similar graphs). As to the quantity of electricity passed corresponding to this current peak, it may be concluded that within one such 'passage' of the curve, $\sim 0.05\%$ of the monolayer substance of the electrode surface takes part in the reaction. This current peak is better expressed for the diamond films with a relatively high content of non-diamond carbon, but it is not observed on single-crystal electrodes. According to Martin *et al.*,[32] this peak is due to the oxidation of the non-diamond carbon of the intercrystallite boundaries, which is less resistant to oxidation than the crystalline diamond. No other peculiarities of the electrode behaviour of diamond, which could be attributed to the intercrystallite boundaries, have been revealed.

Note in conclusion that the wide-bandgap diamond-like carbon a-C:H which is usually electrochemically inactive acquires an electrode activity after the incorporation of a sufficiently large quantity ($\sim 10\%$) of platinum into the bulk of film (in the course of its deposition). In the shape of their potentiodynamic curves and the values of kinetic parameters, the a-C:H/Pt electrodes thus obtained resemble qualitatively the polycrystalline (boron-doped) diamond electrodes. For example, in the redox system $Ce^{3+/4+}$ no current peaks in the curves are observed at the Pt level ranging from traces to 1%, but they become well expressed at 12% of platinum; coefficients α and β being equal to 0.13 and 0.18, respectively. The redox reactions are irreversible; they occur under a mixed diffusion-kinetic control and have a moderate overvoltage.[61]

The results obtained point to the possibility of creation of fairly active electrodes from corrosion-resistant carbonaceous materials, *viz.*, synthetic diamond and diamond-like carbon, by incorporating into their bulk rather small quantities of metal catalysts such as platinum.

Platinum can be distributed in a carbon material in the form of individual atoms or clusters depending on the mode of its incorporation.[82] An essential feature is that platinum is not a doping admixture in a-C:H in the sense of this term as used in the physics of semiconductors. Impedance measurements have shown that the Pt admixture does not virtually change the material resistivity. Therefore, it may be suggested that the effect of platinum is of a purely catalytic nature: its atoms on the electrode surface play the role of active sites on which the adsorption and the electrode reaction proceed at high rates.[50,61]

4. Kinetics of inner-sphere reactions. Diamond electrodes in preparative electrolysis and electroanalysis

The evolution of oxygen from water on the anode and hydrogen on the cathode are regarded as the inner-sphere processes. Potentials of these processes restrict the region of 'ideal polarisability' in aqueous solutions of electrolytes (see Fig. 3*a*,*b*). Overvoltage of these reactions increases with higher quality of electrode films. For the anodic evolution of oxygen, the exchange current is 5×10^{-11} A cm^{-2}, transfer coefficient $\beta = 0.25$; for the hydrogen evolution on the cathode the exchange current is 10^{-10} A cm^{-2} and $\alpha = 0.30$ (see Ref. 32).

The region of 'ideal polarisability' may be restricted by decomposition potentials of not only the solvent but also dissolved electrolyte, *e.g.*, halides. The reactions of anodic oxidation of Cl^-, Br^- and I^- ions with the evolution of the corresponding halogens proceed irreversibly and are accompanied by a much higher (by 1 V for Cl^-) overvoltage than on the platinum or graphite electrodes. Most probably, this is associated with low adsorbability of intermediate products (chlorine, bromine and iodine atoms) on the diamond surface, which thus proves to be passive.[78] (The outer-sphere reactions discussed in Section VI.1 occur without adsorption of reagents or intermediate products on the electrode; for this reason, they are insensitive to the poor adsorption capacity of the diamond surface.)

In addition to the above-mentioned processes, the inner-sphere reactions also include oxidations of numerous organic compounds, in which the interphase charge transfer is accompanied by transformations of organic molecules. Polycrystalline diamond electrodes have been used to investigate the anodic oxidation of chloropromazine,[41] ascorbic acid,[84] anthraquinone-2,6-disulfonate[85] and several amines.[86]

One of the most efficient and promising applications of the diamond electrodes is their use for the electroreduction of compounds that are difficult to reduce. For example, the reduction of nitrate and nitrite ions to ammonium has been investigated.[87–89] In an alkaline solution of NO_3^-, the following reaction takes place on a heavily doped electrode (with N_a up to 10^{21} cm^{-3}) under anodic polarisation:

$$NO_3^- + 7H_2O + 8e \longrightarrow NH_4OH + 9OH^- .$$

At a potential of -5 V, the current density reaches 300 mA cm^{-2} but no corrosion of diamond is observed even after a few days of continuous electrolysis.

The most striking feature of this process is that the anodic current efficiency exceeds several-fold the theoretical limit calculated by the equation for the reaction! Attempts were undertaken to rationalise this fact by the occurrence of the conjugated oxidation of silicon (the diamond film was prepared by deposition on a silicon substrate), *e.g.*, through pinholes in the film. However, special experiments on a free-standing diamond film (see Section II) have shown that the current efficiency, though being somewhat decreased, still remained higher than its theoretical level. The reason of this effect is still unclear.

The electrodeposition of metals (Li, Ag, Cu, Pb, Pt, Hg) leading to the formation of a new phase stands somewhat apart. Data on such processes are scanty and rather contradictory. Lead and mercury are deposited as islets a few micrometers in diameter predominantly over the intercrystallite boundaries.[81] According to Li *et al.*,[18,90] lithium is deposited in the same mode with concomitant intercalation into the non-diamond carbon. Observation of the lithium intercalation – deintercalation may be used as a technique for revealing non-diamond inclusions on the surface of diamond films. Finally, there is indirect evidence that the electrodeposition of copper, the first stages of which follow the 'underpotential deposition' mechanism, also takes place on the intercrystallite boundaries.[8]

Electroanalytical methods have been developed on the basis of certain electrochemical reactions on diamond electrodes. Judging from the results of relevant studies,[8,81] the diamond electrode is well-suited for use in the commonly accepted anodic-stripping analysis of solutions for low concentrations of metal ions, which consists in the cathodic deposition of small quantities of metals on an inert working electrode with their subsequent anodic dissolution.

A flow-type thin-layer cell with a diamond electrode has been devised[85,91,92] for the determination of ethylamine, ethylenediamine and other amines, as well as azide ion N_3^-. Such determinations are carried out by injecting a microportion of the solution under study into the electrolyte flow with subsequent recording of the current jump induced by the oxidation of the compound under analysis (Fig. 12). The electrode function is linear in the concentration range of $10^{-2}-10^{-5}$ M; the detection limit, *e.g.*, of azide ion, is 8 nmol l^{-1} (see Ref. 92).

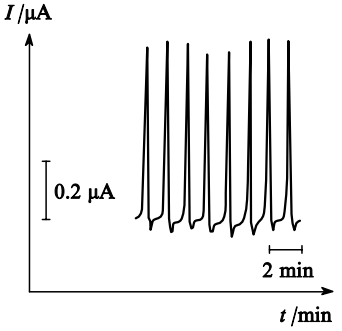


Figure 12. Chronoamperogram in the determination of ethylamine concentration by injecting an aliquot (20 μl of 0.25 mM solution) into a flow-type cell with 0.1 M carbonate buffer; solution flow rate, 0.5 ml min^{-1} (see Ref. 91).

VII. Photoelectrochemistry of diamond

Like any other semiconductor, the diamond demonstrates a photoelectric effect due to photogeneration of free charge carriers upon illumination. An increase in the concentration of charge carriers affects the current across the diamond contact with another conducting phase or the interface charge. In the potentiostatic regime, a photocurrent is recorded and a photopotential is recorded in the galvanostatic and coulombostatic regimes.

Starting from the first study,[11] the photoelectrochemistry of diamond has been investigated by illuminating electrodes with light with quanta energy $h\nu$ smaller than the bandgap ($E_g \simeq 5.5$ eV); this energy is insufficient for the transition of excited electrons from the valence band to the conduction band. Free carriers were apparently formed due to ionisation of some unidentified photosensitive sites in the bandgap of diamond, *viz.*, admixtures or structural defects (the so-called extrinsic or impurity photosensitivity). Curves of photocurrent in the diamond electrode elicited by band-to-band electron transitions (the so-called intrinsic photosensitivity[93]) have been derived quite recently using an excimer laser with a wavelength of 193 nm (which corresponds to quantum energy $h\nu = 6.4$ eV) as the high-energy light source. Figure 13 illustrates well the differences in the photocurrent density j_{ph} in the intrinsic and impurity-related photoexcitations. In the impurity-related excitation the quantum yield of photocurrent was $\sim 0.01\%$,[94] whereas in the intrinsic excitation it reached 34%.[93]

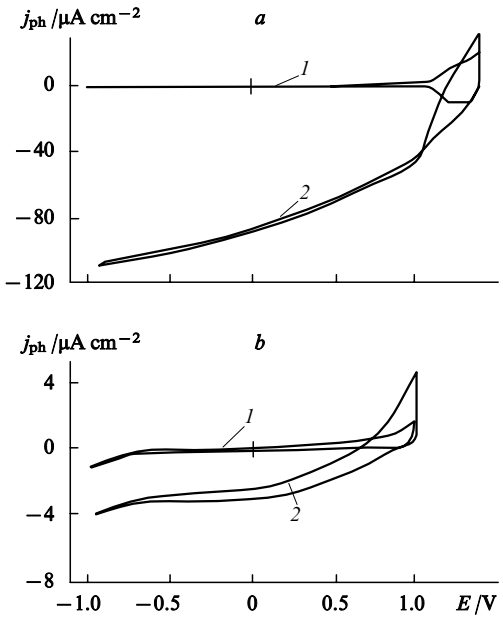


Figure 13. Dependence of dark current (*1*) and photocurrent (*2*) upon illumination of a polycrystalline diamond electrode in 0.1 M KH_2PO_4 under intrinsic (*a*) and impurity-related (*b*) photoexcitation. The quanta energies were 6.4 eV (*a*) and 5 eV (*b*). Density of illumination power was 80 mW cm^{-2} (Ref. 93); the potential values were measured relative to the SCE.

The absolute magnitude of photocurrent is increased with increase in cathodic polarisation. This effect may be understood by examining Fig. 14 showing the square of photocurrent as a function of the potential.[11] This plot is equivalent to the Mott – Schottky plot (see Fig. 5) because, like the latter, it reflects the variation of the width of the space charge layer in the semiconductor diamond as a function of the potential. Upon illumination of this semiconductor, the light-generated charge carriers with opposite signs are separated by an electric field in the space charge region. The minority carriers drift in the electric field

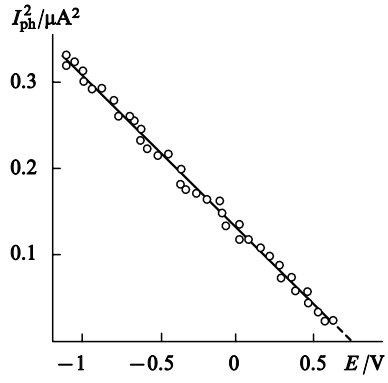


Figure 14. Dependence of the squared photocurrent on the diamond electrode potential in 1 M KCl;[11] the potential values were measured relative to the SCE.

toward the interface, where they are 'captured' by the electrochemical reaction or they charge (in the coulombostatic regime) the electrode, whereas the majority carriers migrate into the bulk of diamond and then, through the ohmic contact, to the external circuit of the electrochemical cell. Therefore, the thicker the space charge layer from which the minority carriers are 'harvested' the stronger the photocurrent. By extrapolating the straight line in Fig. 14 until its intersection with the potential axis, one can determine the flat-band potential in the same way as when using the Mott–Schottky plot; both methods give consistent values for the same electrode (see Section V.1).

In a series of studies [11, 93, 95] the photocurrent was measured in the steady-state mode upon illumination of the electrode with light of constant intensity. Later,[94, 96, 97] pulsed illumination was used; the photopotential and dynamics of its decay were measured after the application of a light pulse. The current of photogenerated minority charge carriers charges the electrode capacitance and thereby determines the potential shift. The analysis conducted with the aid of a somewhat more complex version of the Randles–Ershler circuit (see Fig. 4*b*)‡ afforded a satisfactory description of the dynamics of photopotential decay.

A typical spectrum of the cathodic photocurrent I_{ph} of a diamond electrode is shown in Fig. 15*a*. Processing of such spectra in the coordinates $(I_{ph}h\nu)^{1/2}$ *vs.* $h\nu$ (see Fig. 15*b*) provided values of threshold energies of indirect electron transitions that determine the photogeneration of charge carriers (for more details, see Ref. 6). In some cases, the spectra include two regions and give, respectively, two values of threshold energy. The problem of the elucidation of the physical nature of the energy levels in the bandgap of diamond which participate in such transitions is still far from its solution. Some transitions with a threshold energy close to 4 eV have been identified with the photoexcitation of electrons of the valence band on the energy levels of N^+ ions in the bandgap of diamond localised $\sim$ 1.7 eV below the conduction band.[94]

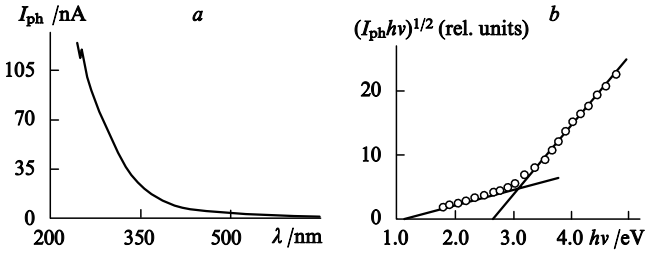


Figure 15. Spectrum of the cathodic photocurrent of a boron-doped polycrystalline diamond electrode in 0.5 M H_2SO_4 under a potential of 0.05 V (relative to NHE) (*a*) and its presentation in the $(I_{ph}h\nu)^{1/2}$ *vs.* $h\nu$ coordinates, which is convenient for the spectrum processing for the threshold energy determination.[94]

The photocurrent–potential curves and the photocurrent spectra were also recorded for the films of amorphous diamond-like carbon.[48, 49, 98] Processing of the spectra similar to that described above has made it possible to determine the width of the mobility gap in the disordered structure of this material. Upon illumination, the diamond-like carbon displays properties characteristic of intrinsic semiconductors.

Photoelectrochemical measurements make it possible to derive certain characteristics of the semiconductor diamond. Thus comparison of the spectra of light absorption coefficient and open-circuit photopotential allowed determination of the diffusion length (2–4 μm) of the minority carriers in polycrystalline diamond films.[99]

‡ The Randles–Ershler circuit was supplemented with a branch which included a capacitance and a resistance connected in series and modelled the process of charging the surface states.

VIII. Conclusion

About ten years have passed since the first studies in the field of diamond electrochemistry. This decade has witnessed the development of a somewhat schematic but rather comprehensive system of concepts of diamond as a novel electrode material. Investigations of diamond electrodes have afforded better understanding of the relationship between the crystal structure of solids and their electrode behaviour.

It is most likely that further studies on diamond electrochemistry will develop both extensively (a wider range of studied reactions, search for new applications of diamond electrodes in fundamental and applied electrochemistry) and intensively (a deeper insight into the relationship between the semiconductor and structural properties of carbon allotropes and their electrochemical behaviour). In the near future, the corrosion-resistant diamond film electrodes may be expected to replace (at least in part) the conventional dimension-stable electrodes based on the platinum group metals, which are used nowadays for the electrochemical synthesis and analysis.

Preparation of this review was supported by the Russian Foundation for Basic Research (Project No. 98-03-32057).

References

1. V S Vavilov, A A Gippius, E A Konorova *Elektronnye i Opticheskie Protsessy v Almaze* (Electronic and Optical Processes in Diamond) (Moscow: Nauka, 1985)
2. J Field (Ed.) *The Properties of Natural and Synthetic Diamond* (London; New York: Academic Press, 1992)
3. K E Spear *J. Am. Ceram. Soc.* **72** 171 (1989)
4. V S Vavilov *Usp. Fiz. Nauk* **167** 17 (1997) [a]
5. V S Vavilov *Usp. Fiz. Nauk* **164** 287 (1994) [a]
6. Yu Ya Gurevich, Yu V Pleskov *Fotoelektrokhimiya Poluprovodnikov* (Photoelectrochemistry of Semiconductors) (Moscow: Nauka, 1983)
7. M Iwaki, S Sato, K Takahashi, H Sakairi *Nucl. Instrum. Methods, Pt II* **209**/**210** 1129 (1983)
8. F Bouamrane, A Tadjeddine, R Tenne, J E Butler, R Kalish, C Levy-Clement *J. Phys. Chem. B* **102** 134 (1998)
9. B Miller, R Kalish, L C Feldman, A Katz, N Moriya, K Short, A E White *J. Electrochem. Soc.* **141** L41 (1994)
10. J Robertson *Adv. Phys.* **35** 317 (1986)
11. Yu V Pleskov, A Ya Sakharova, M D Krotova, L L Bouilov, B V Spitsyn *J. Electroanal. Chem.* **228** 19 (1987)
12. D V Fedoseev, V P Varnin, B V Derjaguin *Usp. Khim.* **53** 753 (1984) [*Russ. Chem. Rev.* **53** 435 (1984)]
13. V P Varnin, in *Tekhnika Sredstv Svyazi (Tekhnologiya Proizvodstva i Oborudovanie)* [Technology of Means of Communication (Production Technology and Equipment)] (Moscow: TsOONTIEKOS, 1989) No. 1, p. 44
14. R Locher, J Wagner, F Fuchs, M Maier, P Gonon, P Koidl *Diam. Relat. Mater.* **4** 678 (1995)
15. M Werner, R Job, A Zaitsev, W R Fahrner, W Seibert, C Johnston, P R Chalker *Phys. Status Solidi A* **154** 385 (1996)
16. P Bou, L Vandenbulcke *J. Electrochem. Soc.* **138** 2991 (1991)
17. K Hashimoto, Y Muraki, R Baba, A Fujishima *J. Electroanal. Chem.* **397** 339 (1995)
18. L-F Li, D A Totir, N Vinokur, B Miller, G Chottiner, E A Evans, J C Angus, D A Scherson *J. Electrochem. Soc.* **145** L85 (1998)
19. P J Fallon, L M Brown *Diam. Relat. Mater.* **2** 1004 (1993)
20. Yu Pleskov, A Tameev, V Varnin, I Teremetskaya, A Baranov *Fiz. Tekhn. Poluprovod.* **31** 1142 (1997)
21. Yu V Pleskov, A R Tameev, V P Varnin, I G Teremetskaya *J. Solid State Chem.* **3** 25 (1998)
22. D M Malta, J A von Windheim, H A Wynands, B A Fox *J. Appl. Phys.* **77** 1536 (1995)

23. M Deguchi, M Kitabatake, T Hirao *Thin Solid Films* **281**/**282** 267 (1996)
24. L S Pan, S Han, D R Kania, M A Plano, M I Landstrass *Diam. Relat. Mater.* **2** 820 (1993)
25. A Ya Sakharova, A E Sevast'yanov, Yu V Pleskov, G L Teplitskaya, V V Surikov, A A Voloshin *Elektrokhimiya* **27** 263 (1991) [b]
26. N G Bukun, E A Ukshe, E I Moskvina, A E Ukshe *Elektrokhimiya* **21** 269 (1985) [b]
27. G A Sokolina, A A Botev, L L Builov, S V Bantsekov, O I Lazareva, A F Belyanin *Fiz. Tekhn. Poluprovod.* **24** 175 (1990)
28. S Nath, J I B Wilson *Diam. Relat. Mater.* **5** 65 (1996)
29. Y Muto, T Sugino, K Kobashi, J Shirafuji *Jpn. J. Appl. Phys.* **2 31** L4 (1992)
30. M M Bataineh, D K Reinhard *Diam. Relat. Mater.* **6** 1689 (1997)
31. T Yano, D A Tryk, K Hashimoto, A Fujishima *J. Electrochem. Soc.* **145** 1870 (1998)
32. H B Martin, A Argoitia, U Landau, A B Anderson, J C Angus *J. Electrochem. Soc.* **143** L133 (1996)
33. G M Swain, A B Anderson, J C Angus *Mater. Res. Bull.* **23** 56 (1998)
34. J W Strojek, M C Granger, G M Swain, T Dallas, M W Holtz *Anal. Chem.* **68** 2031 (1996)
35. G M Swain *J. Electrochem. Soc.* **141** 3382 (1994)
36. Q Chen, M Granger, T E Lister, G M Swain *J. Electrochem. Soc.* **144** 3806 (1997)
37. R DeClements, G M Swain *J. Electrochem. Soc.* **144** 856 (1997)
38. P U Natishan, A Morrish *Mater. Res.* **8** 269 (1989)
39. I Garsia, A Conde, J J de Danborenea, A J Vazquez *Thin Solid Films* **310** 217 (1997)
40. R Ramesham, M F Rose *Corros. Sci.* **39** 2019 (1997)
41. C H Goeting, F Jones, J S Foord, J C Eklund, F Marken, R G Compton, P R Chalker, C Johnston *J. Electroanal. Chem.* **442** 207 (1997)
42. R Ramesham, M F Rose *Diam. Relat. Mater.* **6** 17 (1997)
43. R Ramesham, M F Rose *Thin Solid Films* **300** 144 (1997)
44. R Ramesham, M F Rose *Thin Solid Films* **315** 222 (1998)
45. E P Smirnov, O G Taushkanova, V B Aleskovskii *Dokl. Akad. Nauk SSSR* **290** 901 (1986) [c]
46. P E Pehrsson, M Marchywka, J P Long, J E Butler, in *Applications of Diamond Films and Related Materials (Proceedings of the 3rd International Conference), Gaitherburg, MD, 1995* p. 267
47. A T Howe *J. Electrochem. Soc.* **134** 2470 (1987)
48. A Ya Sakharova, Yu V Pleskov, F Di Quarto, S Piazza, C Sunseri, S S Gerasimovich, V V Sleptsov *J. Electroanal. Chem.* **398** 13 (1995)
49. A Ya Sakharova, Yu V Pleskov, F Di Quarto, S Piazza, C Sunseri, S S Gerasimovich, V V Sleptsov *Elektrokhimiya* **32** 1298 (1996) [b]
50. M D Krotova, Yu E Evstefeeva, Yu V Pleskov, V V Elkin, A M Baranov *Elektrokhimiya* **34** 1039 (1998) [b]
51. Z B Stojnov, B M Grafov, B Savova-Stojnova, V V Elkin *Elektrokhimicheskii Impedans* (Electrochemical Impedance) (Moscow: Nauka, 1991)
52. A Ya Sakharova, Yu V Pleskov, F Di Quarto, S Piazza, C Sunseri, I G Teremetskaya, V P Varnin *J. Electrochem. Soc.* **142** 2704 (1995)
53. W P Kang, Y Gurbuz, J L Davidson, D V Kerns *J. Electrochem. Soc.* **141** 2231 (1994)
54. J A von Windheim, V Venkatesan, D M Malta, K Das *Diam. Relat. Mater.* **2** 841 (1993)
55. Yu E Evstefeeva, M D Krotova, Yu V Pleskov, V V Elkin, V P Varnin, I G Teremetskaya *Elektrokhimiya* **34** 1171 (1998) [b]
56. A Sakharova, L Nyikos, Yu Pleskov *Electrochim. Acta* **37** 973 (1992)
57. Yu V Pleskov, V Ya Mishuk, M A Abaturov, V V Elkin, M D Krotova, V P Varnin, I G Teremetskaya *J. Electroanal. Chem.* **396** 227 (1995)
58. R Ramesham *Thin Solid Films* **322** 158 (1998)
59. Yu V Pleskov, V Ya Mishuk, M A Abaturov, V V Elkin, M D Krotova, V P Varnin, I G Teremetskaya *Elektrokhimiya* **33** 67 (1997) [b]
60. B A Boukamp *Solid State Ion.* **20** 31 (1986)
61. Yu V Pleskov, Yu E Evstefeeva, M D Krotova, V V Elkin, A M Baranov, A P Dement'ev *Diam. Relat. Mater.* **8** 64 (1999)
62. Yu V Pleskov, V V Elkin, M A Abaturov, M D Krotova, V Ya Mishuk, V P Varnin, I G Teremetskaya *J. Electroanal. Chem.* **413** 105 (1996)
63. Yu E Evstefeeva, M D Krotova, Yu V Pleskov, V A Laptev *Elektrokhimiya* **35** 138 (1999) [b]
64. Yu V Pleskov, Yu E Evstefeeva, M D Krotova, V A Laptev *Electrochim. Acta* (1999) (in the press)
65. M A Abaturov, V V Elkin, M D Krotova, V Ya Mishuk, A Ya Sakharova, Yu V Pleskov *Elektrokhimiya* **31** 1214 (1995) [b]
66. G Oskam, D Vanmaekelbergh, J J Kelly *J. Electroanal. Chem.* **315** 65 (1991)
67. E C Dutoit, R L van Meirhaeghe, F Cardon, W P Gomes *Ber. Bunsenges. Phys. Chem.* **79** 1206 (1975)
68. J F McCann, S P S Badwal *J. Electrochem. Soc.* **129** 551 (1982)
69. Yu E Evstefeeva, M D Krotova, Yu V Pleskov, V M Mazin, V V Elkin, V Ya Mishuk, V P Varnin, I G Teremetskaya *Elektrokhimiya* **34** 1493 (1998) [b]
70. T Paikossy, in *The 1997 Joint Meeting of ECS (192nd) and ISE (48th) (Abstracts of Reports), Paris, 1997* p. 972
71. P Delahay *New Instrumental Methods in Electrochemistry* (New York: Interscience, 1954)
72. Z Galus *Teoretyczne Podstavy Electroanalizy Chemicznej* (Warszawa: Panstwowe Wydawnictwo Naukowo, 1971)
73. J Xu, M C Granger, Q Chen, J W Strojek, T E Lister, G M Swain *Anal. Chem.* **69** 591A (1997)
74. G M Swain, R Ramesham *Anal. Chem.* **65** 345 (1993)
75. Yu E Evstefeeva, Yu V Pleskov, V P Varnin, I G Teremetskaya *Elektrokhimiya* **34** 234 (1998) [b]
76. Y Maeda, K Sato, R Ramaraj, D A Tryk,A Fujishima *Electrochim. Acta* (1999) (in the press)
77. S Alehashem, F Chambers, J W Strojek, G M Swain, R Ramesham *Anal. Chem.* **67** 2812 (1995)
78. N Vinokur, B Miller, Y Avyigal, R Kalish *J. Electrochem. Soc.* **143** L238 (1996)
79. R Ramesham, M F Rose *J. Mater. Sci. Lett.* **16** 1693 (1997)
80. A D Modestov, Yu V Pleskov, V P Varnin, I G Teremetskaya *Elektrokhimiya* **33** 60 (1997) [b]
81. M Awada, J W Strojek, G M Swain *J. Electrochem. Soc.* **142** L42 (1995)
82. K I Schiffmann *Mikrochim. Acta* **125** 107 (1997)
83. A D Modestov, Yu E Evstefeeva, Yu V Pleskov, V M Mazin, V P Varnin, I G Teremetskaya *J. Electroanal. Chem.* **431** 211 (1997)
84. R DeClements, G M Swain, T Dallas, M W Holtz, R Herrik III, J L Stickney *Langmuir* **12** 6578 (1996)
85. J Xu, Q Chen, G M Swain *Anal. Chem.* **70** 3146 (1998)
86. M D Koppang, J Blau, G M Swain *Anal. Chem.* (1999) (in the press)
87. R Tenne, K Patel, K Hashimoto, A Fujishima *J. Electroanal. Chem.* **347** 409 (1993)
88. C Reuben, E Galun, H Cohen, R Tenne, R Kalish, Y Muraki, K Hashimoto, A Fujishima, J M Butler, C Levy-Clement *J. Electroanal. Chem.* **396** 233 (1995)
89. F Bouamrane, A Tadjeddine, J E Butler, R Tenne, C Levy-Clement *J. Electroanal. Chem.* **405** 95 (1996)
90. L-F Li, D Totir, B Miller, G Chottiner, A Argoitia, J C Angus, D Scherson *J. Am. Chem. Soc.* **119** 7875 (1997)
91. S Jolley, M Koppang, T Jackson, G M Swain *Anal. Chem.* **69** 4099 (1997)
92. J Xu, G M Swain *Anal. Chem.* **70** 1502 (1998)
93. L Boonma, T Yano, D A Tryk, K Hashimoto, A Fujishima *J. Electrochem. Soc.* **144** L142 (1997)
94. A Ya Sakharova, Yu V Pleskov, F Di Quarto, S Piazza, C Sunseri, I G Teremetskaya, V P Varnin *Elektrokhimiya* **31** 188 (1995) [b]
95. Yu V Pleskov, V P Varnin, I G Teremetskaya, A V Churikov *J. Electrochem. Soc.* **144** 175 (1997)
96. Yu V Pleskov *J. Chem. Vapor Depos.* **5** 126 (1996)
97. Yu V Pleskov, A Ya Sakharova, A V Churikov, V P Varnin, I G Teremetskaya *Elektrokhimiya* **32** 1164 (1996) [b]
98. A Pinkowski, U Stimming, J Winter *J. Electrochem. Soc.* **136** 1849 (1989)
99. Yu V Pleskov, A Ya Sakharova, E V Kasatkin, V A Shepelin *J. Electroanal. Chem.* **344** 401 (1993)

[a] — *Uspekhi-Physics (Engl. Transl.)*
[b] — *Russ. J. Electrochem. (Engl. Transl.)*
[c] — *Dokl. Chem. Technol., Dokl. Chem. (Engl. Transl.)*